Monte Carlo study of the multicharged U(1) Higgs model with radial degrees of freedom

A. Tarancón
Departamento de Física Teórica, Facultad de Ciencias, Universidad de Zaragoza, Zaragoza, Spain
(Received 22 December 1986; revised manuscript received 7 July 1987)

In the lattice U(1) gauge-Higgs model with radial degrees of freedom, a phase-transition point appears in the $\beta=0$ axis for small λ, independent of the charge q of the Higgs fields. Then, with relation to the model without radial degrees of freedom, new phases appear in the (β,J) phase diagram, whose location and order of corresponding phase transitions are studied by a Monte Carlo simulation. We also investigate the existence or nonexistence of free charge in all phases by using analytical and numerical methods.

I. INTRODUCTION

The study of the gauge-Higgs models in the lattice is a first step toward the establishment of the existence or nonexistence of an appropriate continuum limit.[1,2]

The phase diagram of the U(1) gauge-Higgs model with *constant modulus* is well known for different values of the charge q of the Higgs fields.[3] The effect of the introduction of the radial degree of freedom for the Higgs fields has been studied in the model with $q=1$, showing that for λ sufficiently small (λ being the Φ^4 coupling and J the gauge-Higgs coupling as defined in Sec. II), the transition line between the confining and Higgs phases does not end, but rather intersects the $\beta=0$ axis.[4,5] As noted in Ref. 6 this transition point in the $\beta=0$ axis is q independent and therefore new phases must appear in the phase diagram for any other q in relation to the phases in the model without radial degrees of freedom, which are plotted in Fig. 1 ($q=2$ and $q=6$ with $\lambda=\infty$). Here we study the phase diagram of the U(1) gauge-Higgs model with radial degrees of freedom, for $q=2$ and $q=6$ and the order of its phase transitions.

It is also interesting to know in which phases one has or does not have free charge. It is well known[7] that the asymptotic behavior of the Wilson loop expectation value for Yang-Mills lattice gauge theories ceases to be a good order parameter for confinement when the interaction with matter fields is switched on. Indeed, for $q=1$, the screening effects induced by the matter-field fluctuations force the Wilson loop to follow the perimeter law, which rules it out as a good order parameter and, for $q>1$, the Wilson loop behavior turns out to be a good confinement criterion but for *nondynamical charge,* i.e., for the case of the external fractional charge.[8] For the dynamical charge (and then of charge q) the Fredenhagen and Marcu (FM) parameter[9] is a clear criterion of confinement sufficiently tested in several models: Z_2-Higgs model,[10,11] the Schwinger model,[12] the SU(2)-Higgs model,[13] and the U(1)-Higgs model with $q=1$ and 2 (Refs. 6 and 14).

The behavior of the Wilson loop and that of the FM parameter for the Higgs (β and J large), confining (β and J small), and Coulomb (β large, J small) phases of the model studied in this work can be read directly from the corresponding behavior in the study of the U(1) gauge-Higgs model made in Ref. 6. *Here we study (for $q=2$ and 6) the behavior of those two parameters in the new phases which arise when one defrosts the radial degree of freedom.*

This paper is organized as follows. In Sec. II we introduce the model and the observables to be computed and show the occurrence of a phase transition in the $\beta=0$ axis for $\lambda\leq\lambda_c$ and any q. In Sec. III we will describe the Monte Carlo simulation to discuss the resulting phase diagram in Sec. IV. In Sec. V we use analytical and numerical results, to study the existence or nonexistence of free charge. We finish this work with a concluding section.

II. MODEL, LIMIT MODELS, AND OBSERVABLES

The partition function of the Abelian Higgs model in a hypercubical lattice in four dimensions with Higgs fields of charge q is

$$Z(\beta,J,\lambda)=\int\prod_{\mu,\nu}dU_\mu(n)\prod_n d\Phi(n)\exp(S[U,\Phi])\ , \tag{2.1}$$

with S defined as

$$S[U,\Phi]=\tfrac{1}{2}\beta\sum_{\mu,\nu,n}[U_{\mu\nu}(n)+U^\dagger_{\mu\nu}+(n)] +\tfrac{1}{2}J\sum_{\mu,n}[\Phi(n)U^q_\mu(n)\Phi^\dagger(n+\mu) +\text{c.c.}]-V(\Phi)\ , \tag{2.2}$$

where β is the gauge coupling constant,

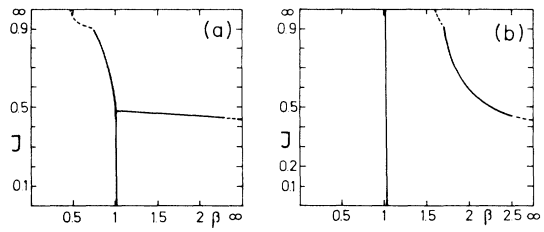

FIG. 1. Phase diagram for the U(1) gauge-Higgs model at $\lambda=\infty$: (a) $q=2$; (b) $q=6$.

$$V(\Phi)=\sum_n V(\Phi(n))$$
$$=\sum_n\{|\Phi(n)|^2+\lambda[|\Phi(n)|^2-1]^2\} \quad (2.3)$$

and

$$\Phi(n)=\rho(n)\phi(n)=\rho(n)\exp[i\chi(n)]\ ,$$
$$\rho(n)\in[0,\infty),\phi(n)\in(0,2\pi]\ . \quad (2.4)$$

In (2.1) $dU_\mu(n)$ is the Haar measure of the U(1) group, and

$$\int d\Phi(n)=\int_{0,\infty}\rho(n)d\rho(n)(\tfrac{1}{2}\pi)\int_{0,2\pi}d\chi(n)\ . \quad (2.5)$$

The notation is standard: μ is a unitary vector in the μ positive direction ($\mu=1,2,3,4$), $n\in Z^4$ labels the site, and $U_{\mu\nu}(n)$ stands for the plaquette.

The action (2.2) represents Higgs fields of charge q because when a local gauge transformation is made

$$U_\mu(n)\to V(n)U_\mu(n)V^\dagger(n+\mu)\ , \quad (2.6)$$

with $V(n)\in U(1)$ and $U_\mu(n)=\exp[i\theta_\mu(n)]$, to obtain a gauge-invariant action, the Higgs fields must transform as

$$\phi(n)\to\phi(n)V^q(n)\ . \quad (2.7)$$

We call "integer charge" the charge q and "fractionary charge" the charge 1.

Knowledge of the theories which we obtain for the limiting values of the parameters of the original theory is useful in order to study the phase diagram of the model, because whenever we have a transition point for such theories we have a line of phase transition, starting at that point, for the original theory.

In the $J=0$ axis one obtains, for any value of q, a pure gauge theory, with a second-order transition in $\beta=1.1$, separating a confining phase (with area law for the decay of the Wilson loop) and a Coulomb phase (perimeter law).[15]

To study the $J=\infty$ axis, we use the unitary gauge, that is to say, we fix $\chi(n)=0\forall n$, in (2.4). In the $\lambda=\infty$ case [and then from (2.3) $\rho(n)=1$] the interaction term, which is $(J\sum_{n,\mu}\cos q\theta_\mu(n))$, makes the only configurations contributing significantly to Z to be those for which

$$\cos q\theta_\mu(n)=1\forall\mu,n\ , \quad (2.8)$$

so that

$$\theta_\mu(n)=2k\pi/q,\quad k=0,1,\ldots,q-1\ . \quad (2.9)$$

Therefore in the $J=\infty$ axis $U_\mu(n)$ is a Z_q variable, which we denote by $\sigma_\mu(n)$. The partition function is now

$$Z(\beta,J=\infty,\lambda=\infty)$$
$$=\sum_{\sigma_\mu(n)\in Zq}\exp\left[\tfrac{1}{2}\beta\sum_{n,\mu,\nu}[\sigma_{\mu\nu}(n)+\sigma^\dagger_{\mu\nu}(n)]\right]\ , \quad (2.10)$$

and we obtain a Z_q gauge theory, with, for $q=2$, a first-order phase transition at $\beta_c=0.44$, with area law for the Wilson loop for $\beta<\beta_c$ and perimeter law for $\beta>\beta_c$ (Ref. 8). In the $q=6$ case two second-order transition points do exist (in $\beta_1=1$ and $\beta_2=1.6$) with area law for $\beta<\beta_1$ and perimeter law for $\beta>\beta_1$ (Ref. 8). In the case of finite λ (but yet $J=\infty$) the interaction term is

$$J\sum_{n,\mu}\rho(n)\cos[q\theta_\mu(n)]\rho(n+\mu)\ , \quad (2.11)$$

and the dominant configurations in the partition function are those for which

$$\rho(n)=\infty,\theta_\mu(n)=2k\pi/q,\forall n,\mu\ ,$$
$$k=0,1,\ldots,q-1\ , \quad (2.12)$$

which imply, also, a Z_q theory so that the transition points in the $J=\infty$ axis are λ independent.

In the $\beta=\infty$ axis, $U_{\mu\nu}(n)=1,\forall n,\mu$, and then $U_\mu(n)=1$, and we obtain the X-Y model with variable modulus

$$S_{X\text{-}Y}=J\,\mathrm{Re}\sum_{n,\mu}\rho(n)\phi(n)\phi^\dagger(n+\mu)\rho(n+\mu)-V(\rho^2)\ .$$

In this model, at $\lambda=\infty$, a first-order phase transition occurs in $J_c=0.453$: this model has a global symmetry (global gauge transformations for the Higgs fields) which breaks spontaneously for $J>J_c$ ($\langle\Phi\rangle\neq0$), and the correlation function for the Higgs fields has two clearly different behaviors. For $J>J_c$,

$$\langle\phi(0)\phi^\dagger(r)\rangle\underset{|r|\to\infty}{\sim}C\langle\phi\rangle\exp(\mathrm{const}/|r|^{d-2})\ ,$$

and, for $J<J_c$,

$$\langle\phi(0)\phi^\dagger(r)\rangle\underset{|r|\to\infty}{\sim}C\exp(-|r|/\xi)\ ,$$

with ξ the correlation length.[8]

Last, we study the $\beta=0$ axis. The partition function (2.1) for $\beta=0$ becomes, in the unitary gauge,

$$Z(\beta=0,J,\lambda)=\int[d\theta_\mu(n)/2\pi][\rho(n)d\rho(n)]\exp\left[J\sum_{n,\mu}\{\rho(n)\cos[q\theta_\mu(n)]\rho(n+\mu)\}-V(\rho^2)\right]\ , \quad (2.13)$$

where $\theta_\mu(n)$ play the role of an external field which can be exactly integrated

$$(\tfrac{1}{2}\pi)\int_{0,2\pi}d\theta_\mu(n)\exp(J\{\rho(n)\cos[q\theta_\mu(n)]\rho(n+\mu)\})=I_0(J\rho(n)\rho(n+\mu))\ , \quad (2.14)$$

with I_0 the modified Bessel function. This expression is q independent. Then the property of analyticity of Z is also q independent; as for $q=1$ Z is nonanalytic,[3,4] the same would happen for any value of q.

To understand the occurrence of this last phase transition let us consider the partition function after the $U_\mu(n)$ integration

$$Z(\beta=0,J,\lambda)=\int [\rho(n)d\rho(n)]\exp\left[\sum_{n,\mu}\ln[I_0(J\rho(n)\rho(n+\mu))]-V(\rho^2)\right] . \tag{2.15}$$

To study the qualitative behavior of this effective action, we recall the asymptotic behavior of the Bessel functions for small and large values of their argument:

$$I_0(x)\underset{x\to 0}{\sim}1+\tfrac{1}{4}x^2 , \tag{2.16}$$

$$I_0(x)\underset{x\to\infty}{\sim}(2\pi x)^{-1/2}e^x , \tag{2.17}$$

with $x=J\rho(n)\rho(n+\mu)$ in our case. For $\lambda\to\infty$ (in practice for $\lambda>0.2$) the $\rho(n)$ field configurations giving a significant contribution to Z are close to 1 (in the $\lambda=\infty$ model we have a Higgs field without radial degrees of freedom), and, then, when J increases from J close to zero to large J (and therefore so increases the I_0 argument), we move *slowly* to a behavior as (2.17) and no phase transition occurs. For $\lambda\to 0$ (in practice for $\lambda<0.1$) the $\rho(n)$ field configurations can be very different from 1, and, then, for increasing J, the Bessel function argument grows rapidly so that the I_0 behavior changes quickly from (2.16) to (2.17), giving rise to a phase transition. *This image is supported by our Monte Carlo simulation, which shows a first-order phase transition at* $J=J_c$ for $\lambda\le\lambda_c$ [$\lambda_c=0.1$] (Ref. 16).

Up to now we have studied only the limit models. To study the full phase diagram of the multicharged U(1)-Higgs model with radial degrees of freedom, we must, of course, resort to Monte Carlo computations of the Wilson loop [for the case $q>1$ (Ref. 8)] and of thermodynamical functions, as the plaquette energy

$$E_p=1-\{2/[d(d-1)]\}(\partial/\partial\beta)\ln Z$$

$$=1-\{2/[d(d-1)]\}\sum_{\mu<\nu}\langle \mathrm{Re}U_{\mu\nu}(n)\rangle , \tag{2.18}$$

and the expectation value of the link

$$L=(1/d)(\partial/\partial J)\ln Z$$

$$=(1/d)\sum_{\mu}\langle \mathrm{Re}\Phi(0)U_\mu^q(0)\Phi^\dagger(0+\mu)\rangle . \tag{2.19}$$

Other interesting quantities are the expectation value of the modulus of the Higgs field[16]

$$M=\langle\rho^2(0)\rangle , \tag{2.20}$$

and the "phase" expectation value of the link

$$N=(1/d)\left\langle\sum_{\mu}\mathrm{Re}\phi(0)U_\mu^q(0)\phi^\dagger(0+\mu)\right\rangle . \tag{2.21}$$

Quantities such as $\langle\Phi\rangle$, $\langle U_{\mu\nu}(n)\rangle$, $\langle U_\mu^q(n)\rangle$ are zero because they are not gauge invariant.

To study the existence of free dynamical charge, we use the FM parameter. We begin denoting by $P_G(L,T)$ a semirectangular path [see Fig. 2(a)] in a space-time plane $0i$, with end points 0 and L in the time-zero axis, and by $P_R(L,T)$ the path defined by $P_R(L,T)=P_G(L,T)\cdot\theta P_G(L,T)$ where θ denotes the reflection through the time-zero axis [see Fig. 2(b)]. We define then

$$G(L,T)=\left\langle\Phi^\dagger(0,0)\left[\prod_{n\in P_G(L,T)}U_\mu^q(n)\right]\Phi(0,R)\right\rangle , \tag{2.22}$$

$$R(L,T)=\left\langle\prod_{n\in P_R(L,T)}U_\mu^q(n)\right\rangle , \tag{2.23}$$

and the FM parameter becomes[9]

$$\sigma=\lim_{L,T\to\infty,L/T\neq 0\text{ fixed}}[\,|G(L,T)|^2/R(L,2T)] . \tag{2.24}$$

The confinement criterion is that if the limit (2.24) is different from zero, confinement occurs. If it is zero it is possible to approximate an isolated quark and there is no confinement.

As noted in Ref. 9, $G(L,T)$ as well as $R(L,T)$ have, asymptotically, an exponential decay with the perimeter, so another way of writing σ is

$$\sigma=\lim_{P\to\infty,L/T\neq 0\text{ fixed}}A[\exp(-C_GP)/\exp(-C_RP)] , \tag{2.25}$$

with $P=2(L+2T)$ and A an irrelevant constant different from zero. In this form σ is manifestly independent of the ratio L/T. Using (2.25), confinement occurs if $C_G=C_R$ and if $C_G>C_R$ it is possible to isolate a charged matter field. As noted in Ref. 15, in order to compute C_G and C_R we need to look for the asymptotic behavior of $C_G(L,T)$ and $C_R(L,T)$, defined by[14]

$$C_G(L,T)=-\tfrac{1}{2}\ln[G(L,T+1)/G(L,T)] \tag{2.26}$$

and

$$C_R(L,T)=-\tfrac{1}{2}\ln[R(L,T+1)/R(L,T)] \tag{2.27}$$

and use any couple of paths with linear distances smaller or equal to one-half of the lattice size (we use periodic boundary conditions). On the contrary, when the confinement criterion is applied using (2.24), the loop entering the denominator must be twice the one entering

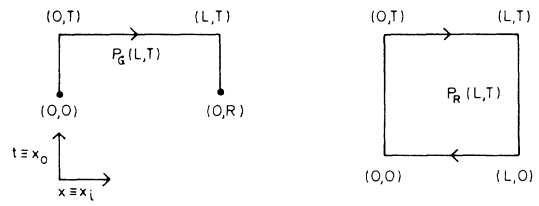

FIG. 2. The paths $P_G(L,T)$ and $P_R(L,T)$ for the operators entering σ.

the numerator which implies (in order to have both inside one-half of the lattice) that, when computing the limit (2.24) a smaller number of points is available than when computing C_G and C_R; therefore, the sensible thing will be to study confinement through the asymptotic behavior of $C_G(L,T)$ and $C_R(L,T)$ (Ref. 14).

III. DESCRIPTION OF THE MONTE CARLO SIMULATION

We use an 8^4 lattice with periodic boundary conditions for both the gauge and Higgs fields. We work in the unitary gauge in order to make the simulation faster. The unitary gauge is problematic in the large β region, because the thermalization of the system is very slow, but in the region of study in this paper ($\beta<4$) there are no problems (we have controlled that thermalization is fast). The continuum group U(1) has been replaced by the discrete Z_{72} in order to obtain a greater speed in the simulation. For $\beta \gg 6$ this substitution is not correct because the theory has a transition not present when the continuum group is used. For our β values this problem is irrelevant and we have checked that the use of greater values of $Z(n)$ does not change the results. For the modulus of the Higgs fields we also use discretized values. Because of the small values of λ which we will study, the modulus of the Higgs fields can be very large and we have controlled that the mean value of $\langle \rho^2 \rangle$ is always much smaller than the maximum of our discretized Higgs fields. We use 2000 different values of $\rho(n)$ which have been arranged as

$$\rho_i(n)=(\rho_{\max}/2000)i, \quad i=1,2,\ldots,2000 , \tag{3.1}$$

with $\rho_{\max}$ between 10 and 20, and carry out one update per $\rho(n)$ variable as follows. An integer random number, ω, is generated between -100 and $+100$ (zero is excluded), and the new tentative variable is defined as

$$\rho_i(n) \rightarrow \rho_{i+\omega}(n) \tag{3.2}$$

with "reflection" boundary conditions.

For the $U_\mu(n)$ update, a U(1) group element G is generated in the neighborhood of the identity, and the new tentative variable is

$$U_\mu(n) \rightarrow G U_\mu(n) . \tag{3.3}$$

Now, because in the large J region $U_\mu(n)$ is "almost" a Z_q variable, in order to improve thermalization, we allow G to be an element of Z_q, otherwise the U(1) variable cannot travel through the entire group because the energy of intermediate configurations is very large.

To compute local observables (E_p, L, etc.) the system was previously thermalized with 100 iterations, and then 400 iterations for measurements, measuring expectation values only every two sweeps through the entire lattice. For nonlocal observables the thermalization is done with 1000 iterations, and then 5000 iterations for measurements, measuring every five sweeps.

IV. PHASE DIAGRAM

To extract the phase diagram we have computed E_p, L, M, and N (2.18)–(2.21) for various λ's, through a return cycle in one parameter (β or J) keeping the other one fixed.

According to the discussion in Sec. II, in the $q=2$ case a "new confining" phase must occur inside the old ($\lambda=\infty$) confining phase. To confirm this, return cycles in J, for fixed β are considered. In the $q=6$ case, two new phases must occur, one inside the old confining phase and the other one inside the old Coulomb phase. To study these phases two types of cycles are considered: (a) J cycles, with β fixed to values in the old confining, Coulomb and large β (Coulomb and Higgs phases) ranges; (b) β cycles, with J fixed to values above and below the transition point, in the $\beta=0$ axis, which turns up for $\lambda \leq \lambda_c$. We repeat these cycles for several λ's between 0.02 and 1.

A. Phase diagram for $q=2$

For λ greater than 0.2 the phase diagram is similar to that of the $\lambda=\infty$ case (except for small numerical differences in the Higgs-Coulomb transition): in the small β region the J cycles have no hysteresis and the thermodynamical functions evolved slowly.

For $\lambda<0.05$ the L, M, and N variables have hysteresis at small β indicating a first-order transition. E_p is constant in practice. In Fig. 3 the values of L in a typical cycle with $\lambda<\lambda_c$ are shown. The phase transition manifests itself by a sudden jump of N from values near zero to values near 1, and another jump of M from 1 to $\rho_{\rm cla}{}^2$, where $\rho_{\rm cla}$ is the minimum of the potential

$$V_{\rm cla}(\rho)=4J\rho^2-\rho^2-\lambda(\rho^2-1)^2+\ln\rho \tag{4.1}$$

whose value, asymptotically (for large J and small λ) is

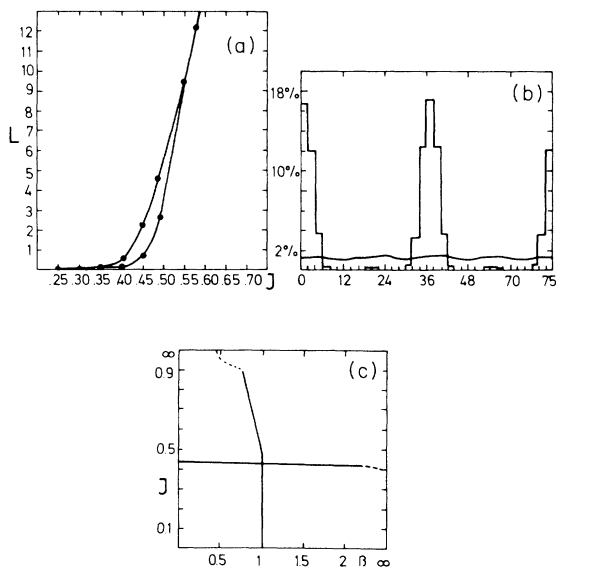

FIG. 3. U(1) gauge-Higgs model with $q=2$ and $\lambda=0.02$. (a) Hysteresis for L at $\beta=0.1$. (b) Frequency of occurrence of U_k at $\beta=0.2$. The histogram stands for a typical configuration close to the equilibrium with $J=0.61$ ($J>J_c$) and the smooth line for $J=0.15$ ($J<J_c$). (c) Phase diagram (the dashed line indicates the extrapolation of the line transition for J or β very large).

$$\rho_{\rm cla}{}^2 \approx (2/\lambda)J \ . \tag{4.2}$$

This behavior is easy to understand. In fact, in the new phase with $J > J_c$, the interaction term in the action (2.1),

$$J\rho(n)\,\mathrm{Re}[U_\mu^q(n)]\rho(n+\mu) \ , \tag{4.3}$$

forces $U_\mu^q(n)$ to be 1, and $\rho(n)$ to be close to $\rho_{\max}$. Then $M \approx \rho_{\max}{}^2$ and the N variable which in the unitary gauge becomes $\langle \mathrm{Re}U_\mu^q(n)\rangle$, is close to 1. When $J \to 0$, the interaction term is negligible for any λ, then the gauge field is random and therefore $N \approx 0$ and $M \approx 1$. To illustrate this point we define the U_k variable for the U(1) group as

$$U_k = \exp[i(2\pi/72)k] , \quad k = 0, \ldots, 72 \ ,$$

and shown in Fig. 3(b) the frequency of occurrence of U_k for two thermalized configurations, in both the $J > J_c$ and $J < J_c$, regions.

The phase diagram for $\lambda < \lambda_c$ is plotted in Fig. 3(c). When λ increases, on the one hand, the transition line between Higgs and Coulomb phases evolved slowly and, on the other hand, in the old confining phase, the transition line evolved toward large values of J, and the intersection with the $\beta = 0$ axis disappears for $\lambda > \lambda_c$.

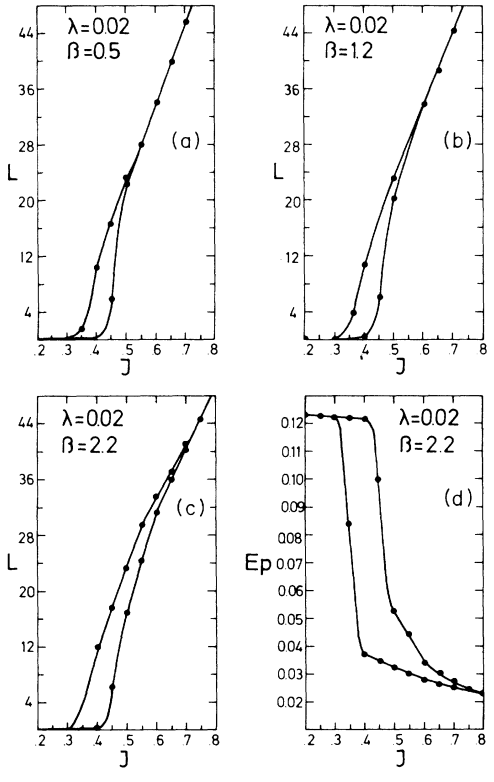

FIG. 4. Hysteresis cycles for the U(1) gauge-Higgs model with $q=6$ and $\lambda=0.02$. (a) J cycle for L with $\beta=0.5$. (b) J cycle for L with $\beta=1.2$. (c) J cycle for L with $\beta=2.2$. (d) J cycle for E_p with $\beta=2.2$.

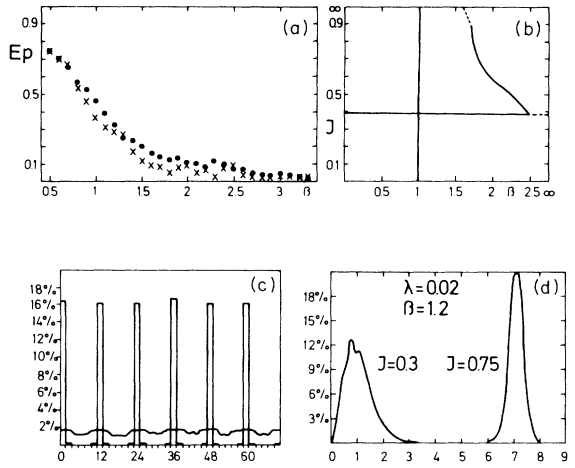

FIG. 5. U(1) gauge Higgs with $q=6$. (a) β cycle for E_p with $J=0.625$ and $\lambda=0.05$. (b) Phase diagram for $\lambda=0.02$. (c) Frequency of U_k: histogram for $\beta=1.2$ and $J=0.75$; smooth line for $\beta=1.2$ and $J=0.3$ ($\lambda=0.02$). (d) Frequency of ρ_i, with the same means and values as in (c).

B. Phase diagram for $q=6$

We shall discuss this diagram for three classes of values of λ: $\lambda < \lambda_c$, intermediate λ (in a sense that will be clear immediately) and large λ ($\lambda > 0.2$). The results for the hysteresis cycles, frequences of occurrence of U_k and ρ_i, and the phase diagrams can be seen in Figs. 4, 5, 6, and 7.

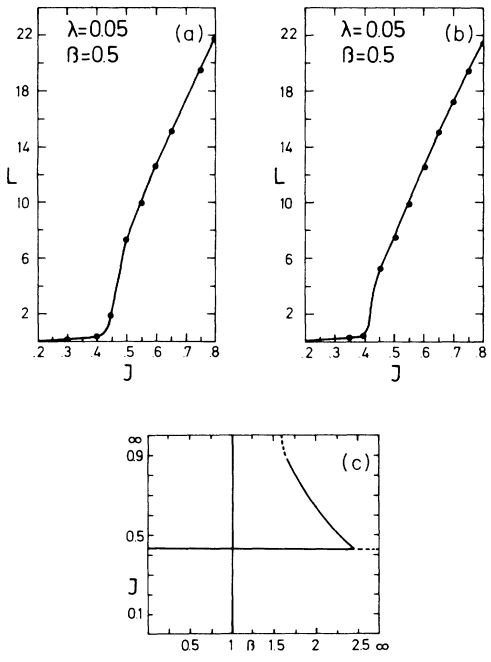

FIG. 6. U(1) gauge-Higgs model with $q=6$ and $\lambda=0.05$. (a) J cycle for L at $\beta=0.5$. (b) J cycle for L at $\beta=1.2$. (c) Phase diagram.

TABLE I. Abstract of the situation for $q=2$, 6, and any λ in the Coulomb, Higgs, and confining phases with $J<J_c$, from the results of Refs. 4 and 11.

Wilson loop decay	Confining phase Area	Coulomb phase Perimeter	Higgs phase Perimeter
σ value	$\neq 0$	$=0$	$\neq 0$
Existence of free fractionary charge	No	Yes	Yes
Existence of dynamical free charge	No	Yes	No

For $\lambda<0.05$, the J cycles for $\beta<1$ (old confining phase) and for $1.1<\beta<1.6$ (old Coulomb phase) present hystereses for L, M, and N (and these hystereses are larger for larger β) and E_p remains almost constant [the results for L are plotted in Fig. 4(a)]. In the Coulomb-Higgs transition all observables present hystereses, including E_p [Figs. 4(c) and 4(d)]. As regards the β cycles, at these values of λ only for E_p and $J>J_c$ we find a very small hysteresis, while L, M, and N remain approximately constant [see Fig. 5(a)].

For increasing λ, the hysteresis in the J cycles decreases very rapidly (more significantly in the small β region). And the new transition line between the two "confining" phases goes up (see Fig. 6). The origin of this transition is the same as in the $q=2$ case: for these λ values and for $J>J_c$, the theory is very close to a Z_6 gauge one [see Fig. 5(c)] and the $\rho(n)$ field is concentrated in the neighborhood of $\rho_{\rm cla}$, while for $J<J_c$, $U_\mu(n)$ is random and $\rho(n)$ is close to 1 [see Fig. 5(d)].

For λ greater than, but close to, λ_c ("intermediate" λ), the transition point is not present in the $\beta=0$ axis, but the old Coulomb phase is still separated in two phases (see Fig. 7).

Lastly, for $\lambda>0.2$ these transition lines disappear and we recover the situation of the $\lambda=\infty$ case [Fig. 1(b)]. We have checked that for $\lambda>0.2$ no phase transition exists for any value of J, i.e., the transition fades out, which makes the new phases to be connected through the λ axis.

V. FREE CHARGE AND CONFINEMENT

As mentioned in Sec. II, the existence of free fractionary and dynamical charges is investigated computing, respectively, the behavior of the Wilson loop and of the FM parameter.

In the $q=2$ case the study has been made in Ref. 6, using strong-coupling and mean-field methods in all phases except in the confining one with $J>J_c$. In Ref. 13 this analysis is completed by a Monte Carlo simulation, which agrees with the analytical results. In Table I

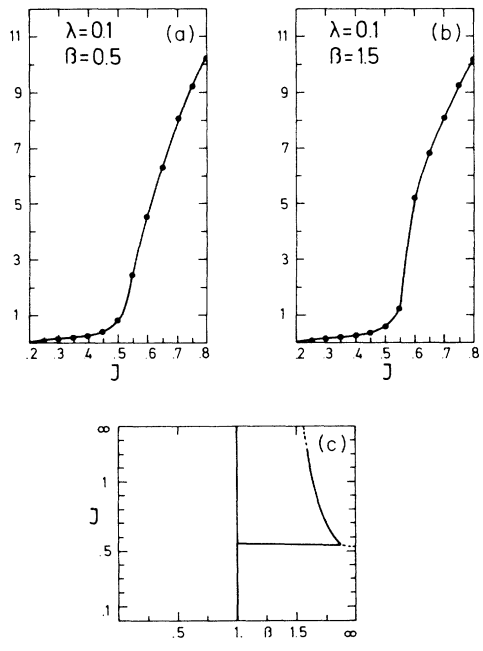

FIG. 7. U(1) gauge-Higgs model with $q=6$ and $\lambda=0.1$. (a) J cycle for L at $\beta=0.5$. (b) J cycle for L at $\beta=1.2$. (c) Phase diagram.

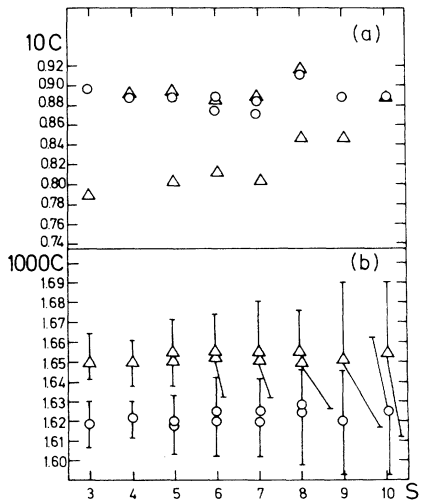

FIG. 8. Numerical values of $10C_G(L,T)$ (circles) and $10C_R(L,T)$ (triangles) versus $S=L+2T$. (a) $q=2$, $\lambda=0.02$, $J=0.61$, $\beta=0.2$. (b) $q=6$, $\lambda=0.02$, $J=0.75$, and $\beta=1.2$. Two circles or triangles at the same value of S correspond to a different combination of L and T. In (a) the size of the symbols is also the error size.

we summarize the results for the $q=2$ case in the Coulomb, Higgs, and confining phases with $J<J_c$.

For $q=6$, in these three phases (in this context Coulomb phase means the old Coulomb phase with $J<J_c$), we obtain, using the strong-coupling and mean-field techniques, the same results as in the $q=2$ case, with small numerical differences.

In this study, the confining phase with $J>J_c$ for $q=2$, and the confining and Coulomb phases also with $J>J_c$ for $q=6$, will be analyzed. To do that, we run a Monte Carlo simulation to compute the Wilson loop and the FM parameter. A point in the parameter space has been considered in each phase. For each one we have run 5000 Monte Carlo iterations per point.

A. $\lambda<0.1, q=2$

The chosen values of the parameters are $\beta=0.2$, $\lambda=0.02$, and $J=0.61$. The Wilson loop behaves as the area, and σ is different from zero. In Fig. 8(a) the values of $C_G(L,T)$ and $C_R(L,T)$ show that asymptotically $C_G=C_R$ and therefore no dynamical free charge exist.

B. $\lambda<0.1, q=6$

(1) Confining phase with $J>J_c$. The simulation is made with the same values of the parameters as in Fig. 5(a), and the result is qualitatively identical. Then no free charge exists, either fractionary or dynamical.

(2) Coulomb phase with $J>J_c$. The Wilson loop decays with the perimeter and $\sigma\neq 0$ with $C_G=C_R$ [Fig. 8(b)]. Then in this phase a fractionary free charge exists, but no dynamical charge.

The perimeter decay of the Wilson loop is obtained only for very large perimeters. This is due to the typical intercharge distance at which screening sets in being close to half the lattice size. Here finite-size effects could start becoming important, so, in order to control this, we have also calculated the expectation value of the Polyakov line, which turns out to be zero within errors and therefore the finite-size effects are small.

Since both Coulomb phases with $J>J_c$ and $J<J_c$ are connected through the λ axis, this result would imply the existence of a frontier, which does not exist when one computes the phase diagram by means of thermodynamical functions, obtained by a finite number of derivatives of the partition function. Yet, since already for the Wilson loop the perimeter behavior is obtained only for large loops, it might well turn out that when L and T increase, different values are obtained for C_G and C_R.

VI. CONCLUDING REMARKS

In this paper we have analyzed the phase diagram of the U(1) gauge-Higgs model with radial degrees of freedom, and charge q of the Higgs field equal to 2 and 6, for a wide range of the β, J, and λ parameters. As pointed out in Ref. 6 the occurrence of a phase transition point in the $\beta=0$ axis for any q produces new phases, which have been studied here by a Monte Carlo simulation. The new phase transitions result to be first order for very small value of λ, and higher order for increasing λ, while the old Coulomb-Higgs transition is always first order.

Also, by using analytical results and performing a Monte Carlo simulation, the existence or nonexistence of free fractionary and dynamical charge has been studied in all phases. Only in the Coulomb phase (and for $J<J_c$, in the $q=6$ case) both free fractionary and dynamical charge, do exist. So in the $q=6$ case the new Coulomb phase is not, in fact, a real Coulomb phase. In the Higgs and the new Coulomb phases only fractionary free charge does exist.

In the remainder phases no free charge exists, either fractionary or dynamical.

We have checked that no important finite-size effects exist, and that the discretization of gauge and Higgs fields is fine enough. The conclusion obtained with relation to the existence or nonexistence of free dynamical charge is based on the asymptotic behavior of the Fredenhagen and Marcu parameter, and it would be interesting to confirm this result for larger perimeters in bigger lattices.

ACKNOWLEDGMENTS

I want to thank V. Alessandrini and J. L. Alonso for their illuminating discussions and very especially J. L. A. for his comments along the writing of this paper. I also acknowledge the financial help of (CACYIT) Comisión Asesora de Investigación Cientificia y Técnica (Plan Movilizador de la Fisica de Altas Energias).

[1]D. J. E. Callaway and R. Petronzio, Nucl. Phys. **B277**, 50 (1986).

[2]W. Langguth, I. Montvay, and P. Weisz, Nucl. Phys. **B277**, 11 (1986).

[3]J. Ranft, J. Kripfganz, and R. Ranft, Phys. Rev. D **28**, 360 (1983).

[4]J. Jersák, in *Advances in Lattice Gauge Theories,* proceedings, Tallahassee, Florida, 1985, edited by D. W. Duke and J. F. Owens (World Scientific, Singapore, 1985), p. 241.

[5]K. Jansen, J. Jersák, C. B. Lang, T. Neuhaus, and G. Vones, Report No. PITHA 85/1, 1985 (unpublished).

[6]V. Alessandrini, J. L. Alonso, A. Cruz, and A. Tarancón, Nucl. Phys. **B281**, 445 (1987).

[7]E. Seiler, *Gauge Theories as a Problem of Constructive Quantum Field Theory and Statistical Mechanics* (Lecture Notes in Physics, Vol. 159) (Springer, Berlin, 1982).

[8]E. Fradkin and S. H. Shenker, Phys. Rev. D **19**, 3682 (1979).

[9]K. Fredenhagen and R. Marcu, Phys. Rev. Lett. **56**, 223 (1986).

[10]K. Fredenhagen and R. Marcu, Commun. Math. Phys. **92**, 81 (1983).

[11]J. Bricmont and J. Frolich, Phys. Lett. **122B**, 73 (1983).

[12]J. L. Alonso and A. Tarancón, Phys. Lett. **165B**, 167 (1985).

[13]H. G. Evertz *et al.,* Phys. Lett. B **175**, 335 (1986).

[14]V. Azcoiti and A. Tarancón, Phys. Lett. B **176**, 153 (1986).

[15]B. Lautrup and M. Nauenberg, Phys. Lett. **95B**, 63 (1980).

[16]G. Koutsumbas, Phys. Lett. **140B**, 379 (1984).